Journal of
Synchrotron Radiation

ISSN 0909-0495

Received 19 April 2011
Accepted 6 September 2011

Titanium local structure in tektite probed by X-ray absorption fine structure spectroscopy

Ling Wang,[a]* Akira Yoshiasa,[a] Maki Okube[b] and Takashi Takeda[c]

[a]Graduate School of Science, Kumamoto University, Kurokami 2-39-1, Kumamoto 860-8555, Japan, [b]Materials and Structure Laboratory, Tokyo Institute of Technology, Yokomama, Kanagawa, Japan, and [c]Nano Ceramics Center, National Institute for Material Science, Tsukuba, Japan. E-mail: wangling.1984@live.cn

The local structure of titanium in tektites from six strewn fields was studied by Ti *K*-edge X-ray absorption near edge structure (XANES) and extended X-ray absorption fine structure (EXAFS) in order to provide quantitative data on Ti—O distance and Ti coordination number. The titanium in tektites possessed different coordination environment types. XANES spectra patterns revealed resemblance to high-temperature TiO_2–SiO_2 glass and TiO_2 anatase. All samples showed that the valence of Ti is 4+. Based on the Ti—O distances, coordination numbers and radial distribution function determined by EXAFS analyses, the tektites were classified into three types: type I, Ti occupies a four-coordinated tetrahedral site with Ti—O distances of 1.84–1.79 Å; type II, Ti occupies a five-coordinated trigonal bipyramidal or tetragonal pyramidal site with Ti—O distances of 1.92–1.89 Å; type III, Ti occupies a six-coordinated octahedral site with Ti—O distances of 2.00–1.96 Å. Although Ti occupies the TiO_6 octahedral site in most titanium minerals under ambient conditions, some tektites have four- and five-coordinated Ti. This study indicated that the local structure of Ti might change in impact events and the following stages.

Keywords: local structure; titanium; XAFS; tektite.

1. Introduction

Tektites are formed at the stage of meteoroid impact, and the concentrations and local structure of each element may hold various kinds of information about such impacts. Tektites are natural silicate glasses which can be found in strewn fields over wide areas. Their formation is widely accepted (Chao, 1993; Glass, 1984; Koeberl, 1986) to be caused by the terrestrial impact theory (Alvarez *et al.*, 1980). Upon a devastating impact of a giant meteoroid on the Earth, particles of the Earth's surface were melted and catapulted into outer space, where they finally solidified and fell back to the Earth; this series of processes is how tektites were formed. Most tektites are several centimetres in diameter and are black, brownish, green and grey in colour. Tektite is the 'driest' rock in the world, a hundred times lower in moisture content than glass of volcanic origin (Beran & Koeberl, 1997). It is an incredible phenomenon, particularly as most collision sites were ocean before the impact events. This suggests that the tektites formed under the most unusual or extreme environments.

Many studies have focused on the Al, Fe oxidation state and coordination number by the XAFS method; fewer studies exist, though, on the titanium local structure in tektites. Glass structure (*i.e.* cation coordination number) is affected by pressure and temperature conditions existing during the glass formation process (Stebbins & McMillan, 1989; Paris *et al.*, 1994; Mysen & Neuville, 1995; Yarger *et al.*, 1995). Frages & Brown (1997) have noted that the XANES spectrum shows Ti in tektite to occupy a four-coordinated site by its pre-edge. EXAFS can be analyzed to give precise information about the bonding distance from Ti to neighbouring atoms. Titanium is a useful probe for obtaining information on the formation of tektites, and XANES and EXAFS studies of the local coordination geometry around Ti in tektite from six strewn fields will provide more comprehensive data. In this study we show that the local structure of Ti in tektite should provide information about the impact event and its subsequent processes.

2. Samples and experiment

The samples that we studied comprised six tektites (Table 1) that came from different strewn fields: hainanite (core and rim parts), indochinite, philippinite and australite from the Australian strewn field; black and grey bediasites from the North American strewn field; and green and brownish moldavites from the European strewn field. In order to analyse the local structure of Ti in tektites, we used the XAFS method. TiO_2 anatase, TiO_2 rutile, $MgTiO_3$ ilmenite, Mg_2TiO_4 spinel, Fe_2TiO_4 spinel and $SrTiO_3$ perovskite were used as the reference compounds.

Ti *K*-edge XAFS measurements were performed at beamline BL-9C, equipped with a Si (111) double-crystal mono-

Table 1
Locations, chemical compositions and colours of the studied tektites.

Sample	Location	SiO_2 (wt%)	TiO_2 (wt%)	Colour
Bediasite-black	Grimes County, Texas, USA	71.9–80.2[a]	0.59–1.05[a]	Black
Bediasite-grey				Grey
Australite	Mount Dare, Northern-most Area, South Australia	70.4–77.2[b]	0.7–0.8[b]	Black
Philippinite	Pagrayanan, Isabela Province, Luzou, Philippines	67.2–74.9[a]	0.5–1.0[a]	Black
Indochinite	Khorat Plateau, Nakhon Ratchasima Province, Thailand	72.9–74.9[a]	0.72–0.89[a]	Black
Hainanite-rim	Hainan Province, China	72.77[c]	0.76[c]	Black
Hainanite-core				
Moldavite-green	Rodomilice Bohemia, Czeck Republic	78.6–82.6[b]	0.3–0.4[b]	Green
Moldavite-brownish				Brownish

[a]Koeberl (1986) and references therein. [b]Heide *et al.* (2001) and references therein. [c]Ho & Chen (1996) (average value).

chromator, of the Photon Factory, KEK, Tsukuba, Japan. The storage ring is operated at an electron energy of 2.5 GeV and ring current of 450 mA. Spectra were recorded in the transmission mode at room temperature near the Ti *K*-edge from 4564.4 to 5355.0 eV with steps from 0.588 to 6.642 eV and 3 s counting time.

The EXAFS function, $\chi(k)$, was extracted from each measured spectrum using the standard procedure (Maeda, 1987). $\chi(k)$ was normalized using MacMaster coefficients according to Lytle *et al.* (1989). In quantitative analyses we carried out a Fourier-filtering technique and a non-linear least-squares fitting method by comparing the observed $\chi(k)_{\rm exp}$ and calculated $\chi(k)_{\rm calc}$. We used the EXAFS formula in the single-scattering theory with the cumulant expansion up to the fourth-order term (Ishii, 1992),

$$\chi(k) = \sum_B \left(N_B/kR_{AB}^2\right)\left|f_B(k;\pi)\right| \exp\left[-2R_{AB}/(k/\pi)\right] \times \exp\left[-2\sigma_2 k^2 + (2/3)\sigma_4 k^4\right] \sin\left\{2kR_{\rm AB} - (2k/R_{AB}) \times \left[1 + 2R_{AB}/(k/\eta)\right]\sigma_2 - (4/3)\sigma_3 k^3 + \psi_{AB}(k)\right\}, \quad (1)$$

where N_B is the coordination number of scattering atom B at a distance R_{AB} from the absorbing atom A, $|f_B(k;\pi)|$ is the backscattering amplitude of photoelectrons, and $\psi_{AB}(k)$ is the phase shift function. Values of the function $|f_B(k;\pi)|$ and $\psi_{AB}(k)$ were calculated using the *FEFF3* program (Rehr *et al.*, 1991). σ_n denotes the nth cumulant. The mean free path λ of the photoelectron was assumed to depend on the wavenumber, $\lambda(k) = k/\eta$, where η is a constant. Analyses of the XAFS data were performed using *XAFS93* programs (Maeda, 1987), whose details are given by Yoshiasa *et al.* (1997). The single-shell fitting was carried out for each nearest-neighbour distance. Because the third- and fourth-order terms in the cumulant expansion were negligible, the final refinement was performed as the harmonic model by the structural parameters R_{AB}, σ_2, η and ΔE_0 values. Here ΔE_0 is the difference between the theoretical and experimental threshold energies. The reliability of fit parameters,

$$R = \sum \left|k_s^3\chi(k_s)_{\rm exp} - k_s^3\chi(k_s)_{\rm calc}\right| / \left|k_s^3\chi(k_s)_{\rm exp}\right|, \quad (2)$$

between the experimental and calculated EXAFS functions was less than 0.063. Fig. 1 shows an example of the $k^3\chi(k)$ signal and Fourier transformation of the Ti *K*-edge EXAFS spectra.

3. Results and discussion

3.1. XANES spectra of tektites

A bound-state transition, such as the $1s \rightarrow 3d$ transition, is primarily responsible for the pre-edge feature of Ti, and is modelled in this formalism as a very large number of scattering events of high order along the same localized path (Brown *et al.*, 1977; Lytle *et al.*, 1988; Frages, 1996*a*). The $p \rightarrow d$ orbital mixing occurs in a site such as Ti located in a TiO_4

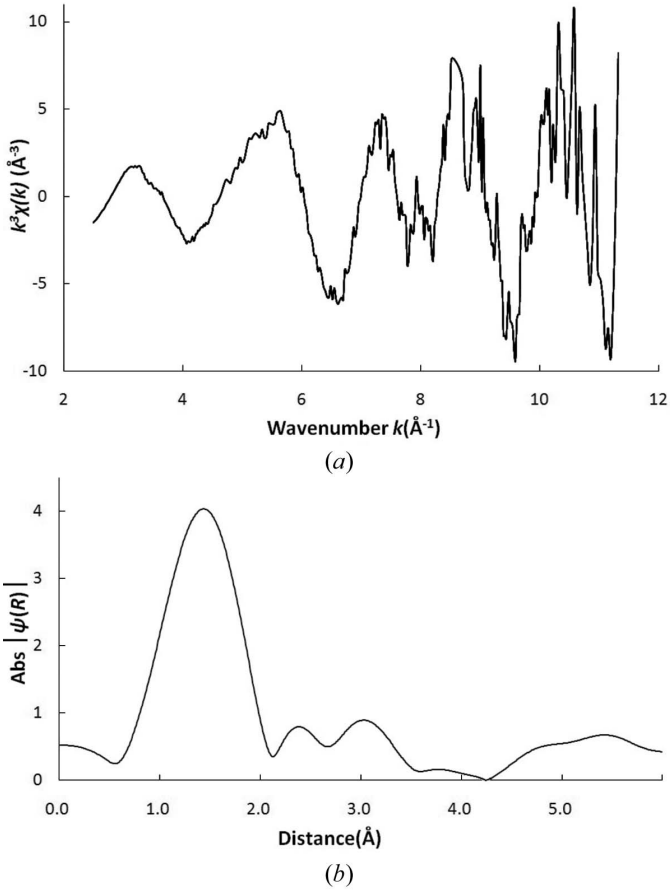

Figure 1
Observed Ti *K*-edge EXAFS $k^3\chi(k)$ oscillation of hainanite in the range $2.5 < k < 11.0$ Å^{-1} (*a*) and its Fourier transform (*b*).

tetrahedron or a TiO_5 square pyramid. The height and position of a pre-edge feature are direct functions of the degree of *p–d* mixing and oxidation state (Wong *et al.*, 1984; Waychunas, 1987; Frages, 1996*b*).

The titanium XANES spectra in tektites are shown in Fig. 2. These spectra are divided into three types according to the pre-edge and XANES shape: type I, indochinite, bediasite-black, moldavite-brownish; type II, hainanite-core, hainanite-rim, australite, philippinite; and type III, moldavite-green. The pre-edge peak heights at 4967.3 eV for types I, II and III are 59–49%, 49–47% and 14%, respectively. The white-line peak and shoulder heights at 4984.7 eV for type I, II and III are around 86%, 90% and 100%, respectively. A detailed comparison of tektite samples from types I and II is shown in Fig. 3. The shoulder heights of hainanite-rim and core (type II) are higher than indochinite (type I) at 4984.7 eV. The XANES spectra in tektites, shown in Figs. 2 and 3, are in agreement

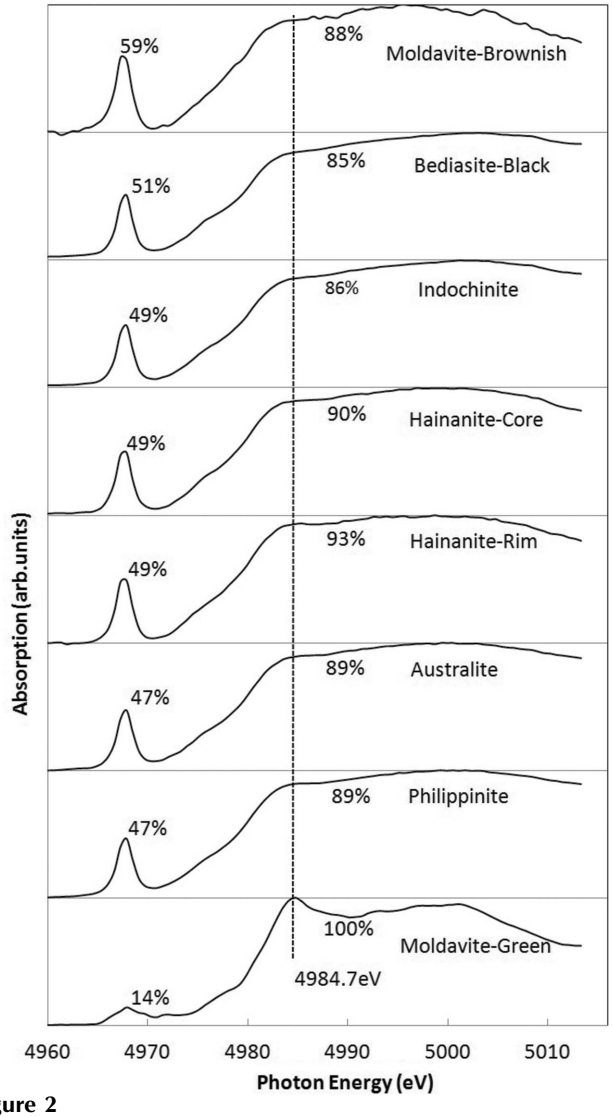

Figure 2
Experimental Ti *K*-edge XANES spectra of tektites. The highest peak position of moldavite-green at 4984.7 eV is shown by a dotted line for comparison purposes. The pre-edge peak heights at 4967.3 eV and pre-edge peak FWHM values change with coordination environment.

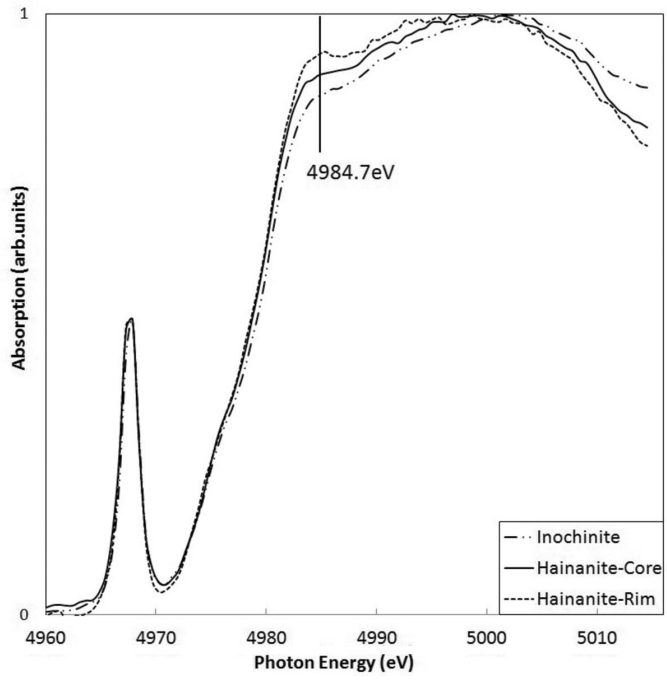

Figure 3
Detailed comparison of typical XANES spectra of indochinite (type I), hainanite-core (type II) and hainanite-rim (type II). The peak position at 4984.7 eV is shown by the solid vertical line for comparison purposes.

with previous studies (Greegor *et al.*, 1984; Yarker *et al.*, 1986; Waychunas, 1987); the pre-edge features are found to be the highest for four-coordinated Ti and lowest for six-coordinated Ti model compounds (Fig. 4). The threshold energy for type II (4978.7 eV) slightly shifts to a lower energy compared with those for type I (4979.3 eV). The distortion of a polyhedron induces a shift of the absorption edge towards lower energy (Paris *et al.*, 1995). Another observation regarding the pre-edge region of our spectra concerns the pre-edge peak full width at half-maximum values (FWHM), which change from 1.8 eV in type I, 1.92 eV in type II to 3 eV in type III. The four-coordinated Ti, for example in Ba_2TiO_4, has a narrow pre-edge peak with a FWHM of 1.5 eV (Greegor *et al.*, 1983). The five-coordinated Ti in glass has a FWHM of 2 eV (Yarker *et al.*, 1986), while the six-coordinated Ti, for example in kaesutite, has a pre-edge peak with a FWHM of 2.7 eV (Galoisy & Calas, 1993).

Fig. 4 compares the observed XANES spectra near the Ti *K*-edge of tektites with reference titanium compounds TiO_2 anatase, TiO_2 rutile, $MgTiO_3$ ilmenite, Mg_2TiO_4 spinel, Fe_2TiO_4 spinel and $SrTiO_3$ perovskite. The threshold edges are located around 4979 eV, which matches to Ti^{4+} in all tektites. Type I and type II have similar features in their spectra to TiO_2–SiO_2 glasses (Frages & Brown, 1997); conversely, the moldavite-green in type III is similar to TiO_2 anatase. TiO_2 anatase and moldavite-green, in which Ti occupies the six-coordinated sites, have the highest peak around 4984.7 eV (position *A*) and a second peak around 5001.1 eV (position *B*). The peak height of position *B* is always more intense than that of position *A* in the other tektites in which Ti occupies five- and four-coordinated sites.

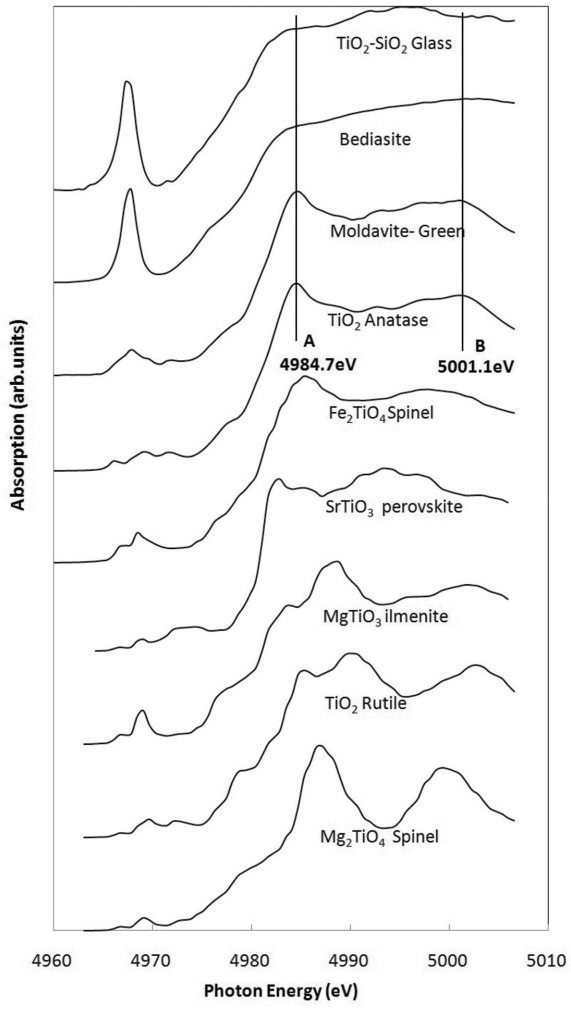

Figure 4
Ti *K*-edge XANES spectra of tektites and reference compounds. TiO_2 anatase and moldavite-green have the highest peak around 4984.7 eV (position *A*) and the second peak around 5001.1 eV (position *B*). The peak height of position *A* is always weaker than those of position *B* in the other tektites in which Ti occupies five- and four-coordinated sites.

3.2. Radial distribution function and local structure

The EXAFS $k^3\chi(k)$ functions were transformed into the radial distribution function (RDF) for the Ti *K*-edge of nine tektites, as shown in Fig. 5. The RDFs of the Ti atoms in indochinite, bediasite-black and moldavite-brownish are similar. Hainanite-rim, hainanite-core, bediasite-grey, australite and philippinite are similar and moldavite-green is discriminated from others. This indicates that each type has the same local atomic environment around the Ti atom.

In order to obtain further information on the structure parameters, we conducted parameter fitting with analytical EXAFS formulae. The obtained structural parameters are summarized in Table 2.

Based on the local Ti—O distances, coordination numbers and RDF determined by EXAFS analyses, we can also classify the tektites into three types. Indochinite, bediasite-black and moldavite-brownish are classified in type I, where Ti occupies a four-coordinated (tetrahedral) site and Ti—O distances are 1.812–1.835 Å. Hainanite-rim, hainanite-core, bediasite-grey, australite and philippinite are in type II, where Ti occupies a five-coordinated (trigonal bi-pyramidal or tetragonal pyramidal) site and Ti—O distances are 1.868–1.921 Å. Moldavite-

Table 2
Structure parameters determined by XAFS.

The expected bonding distances of four-, five- and six-coordinated Ti—O based on the Shannon ionic radii: Ti (four-coordinated)—O = 1.80 Å; Ti (five-coordinated)—O = 1.89 Å; Ti (six-coordinated)—O = 1.99 Å. Uncertainties in the last decimal place are shown in parentheses.

Sample name	σ^2 (Å)	Coordination number	Ti—O distance (Å)	*R*-factor (%)
Indochinite	0.009 (1)	4	1.812 (5)	4.3
Moldavite-brownish	0.020 (1)	4	1.817 (4)	6.3
Bediasite-black	0.004(1)	4	1.835 (3)	0.7
Hainanite-core	0.005 (1)	4 and 5	1.868 (4)	0.3
Hainanite-rim	0.006 (1)	5	1.888 (6)	0.1
Australite	0.002 (1)	5	1.892 (4)	3.5
Bediasite-grey	0.015 (1)	5	1.896 (9)	0.1
Philippinite	0.003 (1)	5 and 6	1.921 (5)	2.7
Moldavite-green	0.003 (1)	6	2.001 (4)	3.5

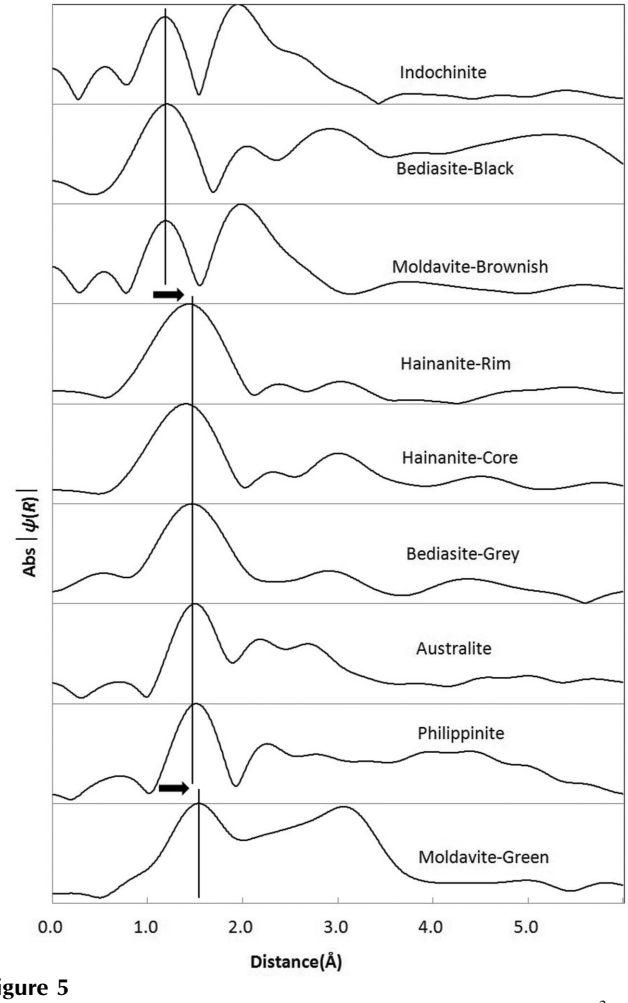

Figure 5
Fourier transforms of the Ti *K*-edge EXAFS oscillation function $k^3\chi(k)$. No phase shift corrections are made. The first nearest peaks corresponding to Ti—O bonds increase with increasing coordination number of Ti in tektite (arrows). Three types can be recognized.

green is in type III, where Ti occupies a six-coordinated (octahedral) site and Ti—O distances are 2.00–1.96 Å.

3.3. Discussion

As the precursor of tektite is primarily of terrestrial origin, the chemical compositions in these tektites are almost identical (Table 1); thus, the composition of the parent rocks is of little importance and it is presumed that different physical conditions at impact events influence the different types of local structures. There are several reasons for the existence of various kinds of local structures. As the tektites splashed out to space and travelled in various routes, they passed through different temperatures and quenching rates. This resulted in various differences in the bonding structure of Ti atoms and arrangements of neighbouring atoms. The local structure of Ti should be closely related to temperature, pressure, quenching rate and size of meteorites and falling melts. These four-, five- and six-coordinated titanium types are formed under diverse atmospheres. According to research on synthetic glass by Paris *et al.* (1994), Frages (1996*c*) and Mysen & Neuville (1995), four-coordinated Ti is formed under high temperature and at low pressure. On the contrary, six-coordinated Ti is formed at lower temperature and at higher pressure. Titanium XANES spectra of synthetic glasses suggest a relatively low coordination number of 4.8 in samples quenched at 5 kbar, and a higher coordination number of 5.8 when quenched at 30 kbar. The decrease in pre-edge intensity from 58% to 29% in glass is consistent with an increase in average coordination number and pressure. A mixture of six-, five- and four-coordinated Ti geometry are present in 1 bar glass and an increasing proportion of six-coordinated Ti occurs in glasses synthesized at progressively higher pressure (Paris *et al.*, 1994). As the pre-edge intensities of tektites are from 59% to 14%, tektites may be formed in a wider pressure range than the pressures previous studies have reported. For instance, tektites in type I may have formed under a pressure of less than 5 kbar, while tektites from type III most likely formed above 30 kbar.

Some differences between the core and rim of hainanite are revealed in the local structure. Wilding *et al.* (1996) performed an experiment on a tektite spheroid of diameter $\sim$40 mm; this exhibited a higher cooling rate on the exterior (10 mm-thick rim, 10 K s^{-1}) than the more massive interior (1 K s^{-1}). The quenching rate difference between the rim and core is sufficient to change the local structure of titanium. This difference in cooling rate is compatible with cooling of the exterior by surface radiation and that of the interior by heat conduction. The Ti—O bonding distance in the hainanite-core is less than that in the hainanite-rim. The quenching rate difference between the rim and core should lead to a change of the local structure of titanium. A higher coordination number favours a faster over a lower quenching rate.

Indochinite, bediasite-black and moldavite-brownish are formed under higher temperature and lower pressure, with a fast quenching rate. The formation environments of temperature, pressure and quenching rates are moderate in hainanite, australite, philippinite and bediasite-grey. Moldavite-green is formed at lower temperatures and higher pressures with a slower quenching rate. In other words, although tektites may be found in the same strewn field, the formation conditions are not equivalent.

Moldavite and bediasite possess two colours; in addition, they have two types of titanium coordination environments, meaning that these glasses were either formed under different physical environments or that they changed later. These features resemble those agates in which a post-heating process changes the local structure around trace elements and results in a more colourful agate. In the case of moldavite and bediasite, the nature of colouration should be addressed in further research.

4. Summary

The local structure of titanium in tektites from six strewn fields was studied by Ti *K*-edge XANES and EXAFS. Based on the Ti—O distances, coordination numbers and radial distribution function determined by EXAFS analyses, we classified the tektites into three types: type I, Ti occupies a four-coordinated tetrahedral site with Ti—O distances of 1.84–1.79 Å; type II, Ti occupies a five-coordinated trigonal bipyramidal or tetragonal pyramidal site with Ti—O distances of 1.92–1.89 Å; type III, Ti occupies a six-coordinated octahedral site with Ti—O distances of 2.00–1.96 Å. Type I and type II have similar features in XANES spectra to TiO_2–SiO_2 glasses and the moldavite-green in type III is similar to TiO_2 anatase. The pre-edge peak heights at 4967.3 eV for types I, II and III are 59–49%, 49–47% and 14%, respectively. The pre-edge peak FWHM values change from 1.8 eV in type I, 1.92 eV in type II to 3 eV in type III. The Ti *K*-edge threshold energy for type II (4978.7 eV) slightly shifts to a lower energy compared with those for type I (4979.3 eV). The chemical compositions in these tektites are almost identical. It is presumed that different physical conditions at impact events influence the different types of local structure. The local structure of Ti should be closely related to temperature, pressure, quenching rate and size of meteorite and falling melts. Type I tektites may have formed under a pressure of less than 5 kbar, while type III tektites most likely formed above 30 kbar. As the quenching rate is lower, a higher coordination number is favoured over a lower one. Moldavite-green is formed at lower temperatures and higher pressures with a slower quenching rate. In other words, although tektites may be found in the same strewn field, the formation conditions are not equivalent.

This study was performed within the Photon Factory Project PAC No.2009G600.

References

Alvarez, L. W., Alvarez, W., Asaro, F. & Michel, H. V. (1980). *Science*, **208**, 1095–1108.
Beran, A. & Koeberl, C. (1997). *Meteorit. Planet. Sci.* **32**, 211–216.
Brown, M., Peierls, R. & Stern, E. A. (1977). *Phys. Rev. B*, **15**, 738–744.

Chao, E. C. T. (1993). *US Geol. Surv. Bull.* **2050**, 22p.
Frages, F. (1996*a*). *Geochim. Cosmochim. Acta*, **60**, 3023–3038.
Frages, F. (1996*b*). *J. Non-Cryst. Solids*, **204**, 53–64.
Frages, F. (1996*c*). *Geochim. Cosmochim. Acta*, **60**, 3055–3065.
Frages, F. & Brown, G. E. (1997). *Geochim. Cosmochim. Acta*, **61**, 1863–1870.
Galoisy, L. & Calas, G. (1993). *Geochim. Cosmochim. Acta*, **57**, 3613–3626.
Glass, B. P. (1984). *J. Non-Cryst. Solids*, **67**, 333–344.
Greegor, R. B., Lytle, F. W., Ewing, R. C. & Haaker, R. F. (1984). *Nucl. Instrum. Methods Phys. Res. B*, **1**, 587–594.
Greegor, R. B., Lytle, F. W., Sandstrom, D. R., Wong, J. & Schultz, P. (1983). *J. Non-Cryst. Solids*, **55**, 27–43.
Heide, K., Heide, G. & Kloess, G. (2001). *Plant. Space Sci.* **49**, 839–844.
Ho, K.-S. & Chen, J.-C. (1996). *J. SE Asian Earth Sci.* **13**, 61–72.
Ishii, T. (1992). *J. Phys. Condens. Matter*, **4**, 8029–8034.
Koeberl, C. (1986). *Annu. Rev. Earth Planet. Sci.* **14**, 323–350.
Lytle, F. W., Greegor, R. B. & Panson, A. J. (1988). *Phys. Rev. B*, **37**, 1550–1562.
Lytle, F. W., Sayers, D. E. & Stern, E. A. (1989). *Physica B*, **158**, 701–722.
Maeda, H. (1987). *J. Phy. Soc. Jpn*, **56**, 2777–2787.
Mysen, B. & Neuville, D. (1995). *Geochim. Cosmochim. Acta*, **59**, 325–342.
Paris, E., Dingwell, D., Seifert, F., Mottana, A. & Romano, C. (1994). *Phys. Chem. Miner.* **21**, 520–525.
Paris, E., Romano, C. & Wu, Z. (1995). *Physica B*, **208–209**, 351–353.
Rehr, J. J., Mustre de Leon, J., Zabinski, S. I. & Albers, R. C. (1991). *J. Am. Chem. Soc.* **113**, 5135–5140.
Stebbins, J. F. & McMillan, P. (1989). *Am. Mineral.* **74**, 965–968.
Waychunas, G. A. (1987). *Am. Mineral.* **72**, 89–101.
Wilding, M., Webb, S. & Dingwell, D. B. (1996). *Geochim. Cosmochim. Acta*, **60**, 1099–1103.
Wong, J., Lytle, F. W., Messmer, R. P. & Maylotte, D. H. (1984). *Phys. Rev. B*, **30**, 5596–5610.
Yarger, J. L., Diefenbacher, J., Smith, K. H., Poe, B. & McMillan, P. F. (1995). *Science*, **270**, 1964–1967.
Yarker, C. A., Johnson, P. A. V., Wright, A. C., Wong, J., Greegor, R. B., Lytle, F. W. & Sinclair, R. N. (1986). *J. Non-Cryst. Solids*, **79**, 117–136.
Yoshiasa, A., Koto, K., Maeda, H. & Ishii, T. (1997). *Jpn. J. Appl. Phys.* **36**, 781–784.